Determinants of BH3 Binding Specificity for Mcl-1 versus Bcl-x[subscript L]

Citation: Dutta, Sanjib et al. "Determinants of BH3 Binding Specificity for Mcl-1 Versus Bcl-x[subscript L]." Journal of Molecular Biology 398.5 (2010): 747–762.

As Published: http://dx.doi.org/10.1016/j.jmb.2010.03.058

Publisher: Elsevier

Persistent URL: http://hdl.handle.net/1721.1/73465

Version: Author's final manuscript: final author's manuscript post peer review, without publisher's formatting or copy editing

Published in final edited form as:
J Mol Biol. 2010 May 21; 398(5): 747–762. doi:10.1016/j.jmb.2010.03.058.

Determinants of BH3 binding specificity for Mcl-1 vs. Bcl-x_L

Sanjib Dutta, **Stefano Gullá**, **T. Scott Chen**, **Emiko Fire**, **Robert A. Grant**, and **Amy E. Keating***
Department of Biology, Massachusetts Institute of Technology, Cambridge, 02139

Abstract

Interactions among Bcl-2 family proteins are important for regulating apoptosis. Pro-survival members of the family interact with pro-apoptotic BH3-only members, inhibiting execution of cell death through the mitochondrial pathway. Structurally, this interaction is mediated by binding of the alpha-helical BH3 region of the pro-apoptotic proteins to a conserved hydrophobic groove on the pro-survival proteins. Native BH3-only proteins exhibit selectivity in binding pro-survival members, as do small molecules that block these interactions. Understanding the sequence and structural basis of interaction specificity in this family is important, as it may allow the prediction of new Bcl-2 family associations and/or the design of new classes of selective inhibitors to serve as reagents or therapeutics. In this work we used two complementary techniques, yeast surface display screening from combinatorial peptide libraries and SPOT peptide array analysis, to elucidate specificity determinants for binding to Bcl-x_L vs. Mcl-1, two prominent pro-survival proteins. We screened a randomized library and identified BH3 peptides that bound to either Mcl-1 or Bcl-x_L selectively, or to both with high affinity. The peptides competed with native ligands for binding into the conserved hydrophobic groove, as illustrated in detail by a crystal structure of a specific peptide bound to Mcl-1. Mcl-1 selective peptides from the screen were highly specific for binding Mcl-1 in preference to Bcl-x_L, Bcl-2, Bcl-w and Bfl-1, whereas Bcl-x_L selective peptides showed some cross-interaction with related proteins Bcl-2 and Bcl-w. Mutational analyses using SPOT arrays revealed the effects of 170 point mutations made in the background of a peptide derived from the BH3 region of Bim, and a simple predictive model constructed using these data explained much of the specificity observed in our Mcl-1 vs. Bcl-x_L binders.

Keywords

interaction specificity; Bcl-2 proteins; BH3 peptides; yeast surface display screening; SPOT array

Introduction

Specific interactions among Bcl-2 family proteins play a crucial role in regulating programmed cell death. The Bcl-2 family can be divided into three classes based on function and on conservation of four Bcl-2-homology (BH) regions. Pro-survival proteins Bcl-x_L, Bcl-w, Bcl-2, Mcl-1 and Bfl-1 share BH regions 1-4, whereas pro-apoptotic proteins Bax and Bak include BH regions 1-3. BH3-only pro-apoptotic proteins such as Bim, Bid, Bad, Puma, Noxa, Hrk and Bmf conserve only the BH3 motif.[1] The pro-apoptotic BH3-only proteins monitor

Corresponding author: Amy E. Keating, 77 Massachusetts Avenue, Building 68-622, Cambridge, Massachusetts 02139, USA, Telephone: (617) 452-3398, Fax: 617-852-6143, keating@mit.edu.

cellular well being and respond to external and internal signals by antagonizing pro-survival Bcl-2 proteins.[2] BH3-only proteins are further classified into sensitizers and activators, based on their ability to induce Bax- or Bak-mediated apoptosis.[3] Small molecules that antagonize pro-survival proteins can also induce apoptosis in tumors and have recently entered clinical trials as promising candidates for anti-cancer therapy.[4; 5]

Structural studies have established a conserved mode of interaction among Bcl-2 family members: the hydrophobic face of an amphipathic helix formed by a BH3 motif inserts into a hydrophobic groove formed by the BH1, BH2 and BH3 regions of pro-survival proteins.[6; 7; 8] This interaction geometry is shared by Bcl-2 family members of low sequence similarity, and BH3 regions from both BH3-only and multi-domain pro-apoptotic proteins can engage pro-survival family members in this way. Thus, an emerging model for how Bcl-2 family proteins control cell death is that pro-survival proteins sequester pro-apoptotic Bax and/or Bak and/or BH3-only activators until these are competitively displaced by BH3-only proteins in response to a pro-death signal.[3; 9; 10; 11] Cancer cells can subvert the apoptotic program by upregulating pro-survival Bcl-2 factors and increasing their capacity to neutralize pro-death signals.[12]

BH3-only proteins exhibit diverse binding specificities for pro-survival Bcl-2 proteins. These are often measured using short peptides corresponding to the BH3 region of BH3-only proteins, for which the affinities of different pro-survival proteins range over 10,000 fold. Most promiscuous are Bim and Puma, which bind to five pro-survival proteins with dissociation constants in the low nanomolar range. In contrast, Bad and Noxa exhibit distinct preferences for some Bcl-2 proteins over others, with Noxa-derived peptides (denoted as Noxa-BH3) binding Mcl-1 and Bfl-1 with nanomolar affinity but showing no detectable binding (>100 μM) to other pro-survival family members, and Bad-BH3 conversely binding with high affinity to Bcl-x_L, Bcl-2 and Bcl-w but not Mcl-1 or Bfl-1.[13; 14; 15] Mechanistically, selective binding profiles mean that only certain combinations of BH3-only proteins are able to kill cells.[13] The distinct binding characteristics of the pro-survival proteins are also relevant for small-molecule therapies that target them. The most effective known inhibitor, ABT-737, is selective for binding to Bcl-x_L, Bcl-2 and Bcl-w[4] and has been shown to bind at the same site as the BH3 peptides.[16] However, cancers that rely on Mcl-1 to evade apoptosis are resistant to ABT-737 and related molecules.[17] This makes it a high priority to identify Mcl-1 specific or Bcl-2-family pan-specific ligands.

Despite the importance of specificity in both the mechanism and treatment of apoptotic mis-regulation in cancer, the sequence and structural determinants of binding specificity in Bcl-2 family members are still not completely understood. A number of studies have systematically addressed determinants of BH3 peptide binding to pro-survival Bcl-2 family members, and a few have addressed differential interactions with Bcl-x_L vs. Mcl-1.[16; 18; 19] Alanine and hydrophile scanning studies have been used to examine the effects of substitutions in several BH3 domains on binding to different pro-survival proteins.[16; 18; 19; 20; 21] Strikingly, it has been demonstrated that Bim-BH3 variants with 2 or even 3 alanine mutations at conserved hydrophobic positions maintain high affinity for binding to Mcl-1 while losing binding affinity for Bcl-x_L.[19] Guided by data generated from alanine and hydrophile scanning, Boersma et al. combined pairs of point substitutions in Bim-BH3 to give peptides with nanomolar affinities for Mcl-1 that discriminated against Bcl-x_L, and vice versa. These mutants achieved >1,000-fold specificity in the case of Mcl-1 binding and ~100-fold specificity in the case of Bcl-x_L binding.[18] These studies offered valuable insights into substitution effects in Bim-BH3.

We have used a combination of experimental and computational methods to further explore the sequence determinants of BH3 interactions with Bcl-x_L vs. Mcl-1. We used yeast surface display [22; 23] to isolate BH3 peptides specific for binding Mcl-1 in preference to Bcl-x_L and vice versa. To better understand interaction specificity determinants in Bim-BH3 and in our

engineered peptides, we used SPOT peptide arrays to characterize Mcl-1 vs. Bcl-x_L binding to hundreds of BH3 peptide mutants.[24] We constructed a simple model that bridges our observations from these two experimental methods and identifies important sequence features that explain much of the binding specificity.

Results

Yeast Surface Display of Bim-BH3 peptide

We used yeast surface display as a platform to study the interactions between human pro-survival proteins and BH3 peptides.[22] We expressed a peptide encompassing 31 residues of the BH3 motif of Bim as a fusion to the yeast cell surface protein Aga2p (Figure 1A). Bim-BH3 is a high affinity interaction partner for both Mcl-1 and Bcl-x_L that has been widely studied; several crystal structures illustrate how it forms complexes with pro-survival proteins.[6; 7; 25] Successful expression of Bim-BH3 on the surface of yeast was confirmed by fluorescence activated cell sorting (FACS), after staining with a primary antibody against a FLAG tag located at the carboxyl terminus of the BH3-peptide and a fluorescein isothiocyanate (FITC) labeled secondary antibody (Figure 1A; Supplemental Figure 1). Binding to pro-survival proteins was detected using an amino terminal c-myc tag on the pro-survival proteins, an anti-c-myc antibody and a phycoerythrein labeled secondary antibody (Figure 1A). In agreement with the strong interactions observed with other *in vitro* techniques,[13; 14; 16; 18] dissociation constants in the low nanomolar range were obtained when yeast cells displaying Bim-BH3 were titrated with soluble Bcl-x_L or Mcl-1 (Supplemental Table 1; Supplemental Figure 2).

Library Construction and Screening

To identify BH3 peptides that bind selectively to different pro-survival proteins, we designed a peptide library based on human Bim-BH3 by introducing diversity at four core and two boundary positions (Figure 1B). BH3 sequences are characterized by the presence of four conserved hydrophobic residues (positions 2d, 3a, 3d and 4a) and a conserved aspartate (position 3f) (Figure 1C). These residues form interactions with pro-survival proteins as illustrated in several high-resolution structures.[6; 7; 8; 21; 26] Mutations in the four hydrophobic positions of Bim-BH3 peptides can confer selectivity for binding to Bcl-x_L or Mcl-1,[16; 18] and the conserved Asp can also be mutated to other residues and retain binding to murine Bcl-x_L.[27] In addition to these five positions, we included position 3b in the library as a structurally interesting boundary position that could potentially impart binding specificity.[6; 7] Previous studies from the Gellman group demonstrated that position 3b can be substituted with uncharged amino acids such as Ala/Gln, though mutation to Glu inhibited binding to both Bcl-x_L and Mcl-1.[18] We randomized these six positions with a subset of amino acids (Supplemental Table 2) to create a combinatorial library that was transformed into yeast to generate ~10^7 individual transformants, exceeding the theoretical library size (8.4×10^5) by greater than 10 fold.

To identify peptides selective for binding to Mcl-1 vs. Bcl-x_L, we imposed positive and negative selection in successive rounds of library enrichment by cell sorting (Figure 1D). For example, to isolate Mcl-1 specific peptides, we carried out successive rounds of screening for binding to Mcl-1 at a concentration of 1 μM. After four rounds, the population showed significant enrichment for binding to Mcl-1 (Supplemental Figure 3A). Interestingly, this population also exhibited some specificity for binding to Mcl-1, as evidenced by weak binding to Bcl-x_L at 1 μM (Supplemental Figure 3B). We then performed three rounds of counter screening against 1 μM Bcl-x_L to eliminate Bcl-x_L binding. The resulting population was finally sorted for binding to Mcl-1 at 10 nM, to identify high affinity Mcl-1 binding peptides that did not bind Bcl-x_L. To confirm specificity, 96 randomly chosen clones from this

population were tested for binding to 10 nM Mcl-1 or 1 μM Bcl-x_L. A significant number (~76%) showed detectable binding to 10 nM Mcl-1 but not to 1 μM Bcl-x_L (Specificity Index S.I. ≥ 2 in Figure 2A, B).

Using a similar scheme, combining positive selection for binding to Bcl-x_L and negative selection against binding to Mcl-1 (Figure 1D), we generated a population of Bcl-x_L binding clones that exhibited specificity for binding to Bcl-x_L (10 nM) over Mcl-1 (1 μM) (Supplemental Figure 4). In addition, to identify BH3 peptides that bound strongly to both Bcl-x_L and Mcl-1, the pool of Mcl-1 binding clones after four rounds of positive screening using 1 μM Mcl-1 was further sorted for binding to Mcl-1 and Bcl-x_L at 10 nM concentration in subsequent steps (Figure 1D). Individual clones from the final population were tested to confirm binding to both Bcl-x_L and Mcl-1 at a concentration of 100 nM.

Sequencing of peptides specific for binding Mcl-1 vs. Bcl-x_L

We sequenced a total of 288 clones (96 from each category), obtaining 33 and 40 tight-binding, unique Mcl-1 and Bcl-x_L specific peptide sequences, respectively, as well as 17 unique sequences for peptides that bound tightly to both Bcl-x_L and Mcl-1 (Supplemental Tables 3, 4 and 5). Figure 2C-F shows sequence logos derived from peptides with different binding properties, as well as a hypothetical logo for the full diversity of the pre-screened library where positions are weighted by codon degeneracy.[28] Many sequences (28 out of 96) in the pool of clones observed to bind to both Bcl-x_L and Mcl-1 corresponded to that of wild-type Bim-BH3. As expected, this sequence did not occur among any of the Mcl-1 or Bcl-x_L specific clones. The sequence logos highlight notable differences between the two specificity classes, predominantly in positions 3a, 3d and 4a. Five of the six randomized positions showed variability; only position 3f was highly conserved (as Asp), in agreement with the multiple sequence alignment of native BH3 motifs (Figure 1C).

Affinities and specificities of engineered BH3 peptides

Five peptides specific for each pro-survival protein were chosen for further characterization, considering both their level of binding to the desired target when displayed on yeast and also sequence diversity in library positions. For these ten clones, we measured K_d values for yeast-displayed peptides that ranged from ~10-70 nM (Supplemental Table 1; Supplemental Figures 5, 6). We also tested these sequences as purified 23-residue synthetic peptides in a fluorescence polarization competition assay for binding to Mcl-1 and Bcl-x_L.[29] We used unlabelled peptides to compete with fluorescently labeled Bim-BH3 and determined the inhibition constant (K_i) using a complete competitive binding model.[30] As a positive control, we measured K_i for an unlabeled Bim-BH3 peptide. Figures 3A and B show the competition binding results for the Mcl-1 and Bcl-x_L specific peptides, respectively. Peptide MB1 had affinity (K_i ~ 4 nM) comparable to wild-type Bim-BH3 (K_i ~ 2 nM) whereas four other Mcl-1 specific peptides (MB2, MB7, MF11, MG1) had weaker affinity. The five Bcl-x_L specific peptides competed effectively with wild-type Bim-BH3 for binding to Bcl-x_L (Figure 3B), with K_i values ranging from ~3-20 nM.

As expected, the peptides identified in yeast screening as selective for Mcl-1 or Bcl-x_L did not exhibit strong binding to Bcl-x_L or Mcl-1, respectively, as indicated by their inability to compete with labeled Bim-BH3 up to a concentration of 10 μM (Figure 3C). Although we counter screened only against Bcl-x_L (or Mcl-1), we also tested peptides for binding to other Bcl-2 family pro-survival proteins. In yeast surface display, the Mcl-1 specific peptides did not exhibit significant binding to Bcl-2 or Bcl-w at a concentration of 1 μM. Mcl-1 is most similar to Bfl-1, with 21.4% sequence identity, yet none of the Mcl-1 specific peptides exhibited binding to 1 μM Bfl-1 either. This selectivity was confirmed in solution competition binding assays, in which the five Mcl-1 specific peptides did not compete with Bim-BH3 for binding

to Bcl-2, Bcl-w or Bfl-1 up to a concentration of 10 μM. In contrast, most Bcl-x_L specific peptides showed cross reactivity with Bcl-2 and Bcl-w in yeast-display experiments. As purified peptides, all five Bcl-x_L specific peptides exhibited binding, albeit weaker, to both Bcl-2 and Bcl-w in the competition binding assay (Figure 3C). This result emphasizes the difficulty of distinguishing between Bcl-x_L, Bcl-2 and Bcl-w. However, none of these peptides competed for binding to Bfl-1.

X-ray crystal structure of a Mcl-1 specific peptide complex

The observation that the novel BH3 variants competed with Bim-BH3 for binding to Mcl-1 and Bcl-x_L confirmed that they bind to the same hydrophobic groove. To investigate details of the interaction further, we determined the crystal structure of the Mcl-1 specific peptide MB7 in complex with Mcl-1 (Figure 4A). MB7 has three changes with respect to Bim-BH3; isoleucine to alanine at 2d (Ile2dAla), leucine to isoleucine at 3a (Leu3aIle) and phenylalanine to asparagine at 4a (Phe4aAsn). The complex crystallized in space group $P2_12_12$ and diffracted to 2.35 Å in the presence of 1 M zinc sulphate, which is similar to the conditions for the crystallization of the wild-type Bim-BH3: Mcl-1 complex.[6; 31] There were two Mcl-1—peptide complexes in the asymmetric unit. The structure of the complex is very similar to that of wild-type Bim-BH3 in complex with Mcl-1, with very small changes in side-chain orientations evident in both the peptide and Mcl-1. The Asn at position 4a is accommodated in a pocket of Mcl-1 that is more open and accessible to solvent than the corresponding region of Bcl-x_L (Figure 4B).[7] There is a shift of Tyr at position 4e to fill the space created by the large-to-small Phe-to-Asn mutation. The Ile2dAla and Leu3aIle mutations also do not lead to any structural change in the peptide backbone, but there is a shift of Leu 235 in Mcl-1 to fill the void created by the Ala mutation at 2d (Figure 4C). This trend of accommodating mutations with rather small changes in Mcl-1 has also been observed for other Bcl-2 family complexes.[19; 20; 32; 31]

SPOT arrays highlight specificity determinants in Bim-BH3

We carried out a substitution analysis of Bim-BH3 peptides in which 10 interface positions (including the six randomized in the yeast library) were mutated – one at a time – to all amino acids excluding Cys and Met (Figure 1B). SPOT arrays displaying 26-residue Bim-BH3 variants were constructed using solid-phase synthesis. Six hundred peptides were printed per four by six inch membrane, allowing the qualitative measurement of binding of hundreds of unique peptides simultaneously. Membranes of 200 spots each, including 170 Bim-BH3 variants, were probed with either 100 nM or 1 μM of Mcl-1 or Bcl-x_L (Figure 5; Supplemental Table 7). The overall reproducibility of the data can be seen in the first column of each array, where every sequence is a repeat of the native. Good reproducibility was also observed for several mutant sequences that appeared 2-3 times on the membranes. Trends observed using 100 nM probe concentration were reproduced at the higher concentration, with additional interactions also becoming apparent. A peptide with Asp at the 3a position (Leu in Bim) was reproducibly observed not to interact with either Mcl-1 or Bcl-x_L on the arrays, consistent with previous reports.[16] Proline-substituted peptides generally bound poorly, although Pro was tolerated at a few N-terminal sites (especially 2d and 2e). The SPOT results agree qualitatively with previously reported binding studies for point mutations made in Bim-BH3 peptides, and with a prior saturating substitution analysis at the 3a and 4a positions carried out using a phage ELISA technique.[16; 18; 19]

Some patterns observed in the substitution arrays were consistent with expectations from sequence conservation in native BH3-only proteins (Figure 1C). For example, the strictly conserved Asp was strongly favored at position 3f for interaction with both Mcl-1 and Bcl-x_L. Position 3e, which is typically occupied by small amino acids in native BH3 sequences, could not tolerate substitution with residues larger than Gly, Ala or Ser on the SPOT arrays,

especially for Mcl-1 binding. The 3a position, which is universally conserved as Leu, generally could not accommodate charged or polar residues in complexes with Bcl-x_L or Mcl-1, although some other hydrophobic residues maintained binding. Bim-BH3 with a Tyr at position 3a showed selective binding to Bcl-x_L but not Mcl-1, consistent with previous observations by Lee et al.[16]

We observed distinct differences between the Mcl-1 vs. Bcl-x_L profiles determined using SPOT arrays. Notably, positions 4a, 2e and 3b were more permissive for Mcl-1 binding compared to Bcl-x_L, whereas the opposite was true for positions 3d, 2d and 3e. At position 4a, most single-site mutants bound to Mcl-1 but not to Bcl-x_L, which clearly exhibited a preference for large hydrophobic residues; this has been previously observed and discussed in the literature.[16; 18; 19] At position 2e, Mcl-1 accommodated a range of amino acids, including Val, Pro and Thr at low probe concentration and all amino acids at higher probe concentration (Figure 5A and C). In contrast, Bcl-x_L had a striking preference for Gly and Ala, with Ser, Thr and Pro additionally allowed at 1 μM probe concentration (Figure 5B and D). Position 3b allowed substitution with negatively charged residues for binding to Mcl-1 at 100 nM, in contrast to Bcl-x_L, and this difference was more pronounced at 1 μM. At position 3d, most substitutions significantly reduced binding to Mcl-1 while maintaining Bcl-x_L binding at 100 nM protein (Figure 5A and B). This pattern was to some extent dampened at 1 μM probe concentration, but the trend was still clear (Figure 5C and D). For position 2d, Bcl-x_L allowed positively charged residues and aromatics, in contrast to Mcl-1, where this position was more constrained to Ile, Val and Ala at low probe concentration. At position 3e, Ala and to a lesser extent Ser, retained binding to Bcl-x_L but reduced binding to Mcl-1. Notably, Bad, a Bcl-x_L specific peptide, has Ser at this position (Figure 1C).

To explore sequence space more broadly, we synthesized combinatorial library SPOT arrays. We identified residues that occurred with high frequency in selected sequences from our yeast-display screening: Ile (wild type), Ala and Phe at position 2d; Leu (wild type), Ile, Phe and Ala at position 3a; Arg (wild type) and Asp at position 3b; Ile (wild type), Phe, Asp, Asn, Ala at position 3d; Phe (wild type), Val and Asn at position 4a. From this reduced library, we synthesized all 360 possible sequences. The resulting membranes, referred to here as library arrays, were probed with 100 nM Mcl-1 or Bcl-x_L. Some interactions of interest are shown in Figure 6A, B and the whole library array is included in Supplemental Figure 7 and quantified in Supplemental Table 8. The library arrays included a wider range of sequence contexts and highlighted specificity determining residues not evident in the Bim-BH3 substitution arrays. This was valuable for model building and interpretation (see below).

SPOT array data capture determinants of Mcl-1 vs. Bcl-x_L binding

Using SPOT data from the Bim-BH3 substitution analysis, we developed a position-specific scoring matrix (PSSM) to capture sequence features characteristic of Mcl-1 vs. Bcl-x_L binding. We defined the score for amino acid i at position j binding to a specific pro-survival protein R, $SR_{i,j}$, by taking the logarithm of the normalized fluorescence intensity for the corresponding Bim point mutant on the membrane. PSSM models were built for both Bcl-x_L and Mcl-1 binding, and only positions and amino acids covered by the SPOT analysis were included in the model.

We used the PSSM to score each of the sequences isolated in yeast-display screening by summing score contributions from the 6 variable positions. As shown in Figure 6E, this simple model does a good job separating sequences with different binding properties. Most of the Bcl-x_L specific sequences had high Bcl-x_L scores and low Mcl-1 scores, whereas the Mcl-1 specific sequences had low Bcl-x_L scores and a range of Mcl-1 scores. Sequences of peptides that bound to both Mcl-1 and Bcl-x_L generally had high Bcl-x_L and Mcl-1 scores. Overall, the analysis shows that information about binding specificity for single point mutants of Bim-BH3, as

captured by the SPOT experiments, can be used to describe the specificities of the engineered sequences with a simple, linear model.

The initial PSSM model performed well, and we explored simple ways in which it could be improved. Although we currently lack the large amount of quantitative data required to describe synergy between peptide positions, even simple PSSM models can potentially be improved by obtaining better estimates of single-position effects. Therefore, we used data from the library arrays to construct a second PSSM, which allowed us to derive mutational scores averaged over multiple contexts for some key substitutions. Evaluating substitutions in multiple contexts also provided a larger dynamic range for the assay. Using the revised PSSM model, we obtained better separation of scores on the Mcl-1 binding axis (Figure 6F). Notably, the percentage of Mcl-1 specific peptides having Mcl-1 scores higher than the highest-scoring Bcl-x_L specific peptide along this axis increased from 33% to 85%. We observed that much of this change was attributable to a significantly more favorable score for Val at 4a binding to Mcl-1, when averaged over the library SPOT sequences. Though this was not obvious from our single-substitution SPOT arrays (Figure 5A), sequences with Val at 4a exhibited significantly enhanced binding to Mcl-1 compared to the wild-type residue Phe in the context of destabilizing mutations at other positions, e.g. Phe, Asp, Asn or Ala at position 3d or Asp at position 3b (Figure 6A, B). Competition binding assays confirmed that a Phe4aVal mutation in Bim-BH3 increased affinity for Mcl-1 more than 10 fold (K_i < 100 pM) while reducing affinity for Bcl-x_L ~30 fold (K_i ~ 30 nM) (Figure 6C and D).

Discussion

We have isolated BH3 peptides specific for binding pro-survival Bcl-2 proteins using yeast-surface display. Using a single-cell sorting technique, we screened for both affinity and specificity and quantified the binding behavior of selected peptides to bind Mcl-1 in preference to Bcl-x_L and vice versa. Specific peptides identified in this way bound their intended targets competitively with known BH3 ligands, and solution studies indicated affinities close to that of wild-type Bim-BH3. Mcl-1 and Bcl-x_L have the lowest sequence identity among the five Bcl-2 family pro-survival proteins and may therefore be considered as the easiest targets to differentiate. Yet the features that discriminate their interaction preferences are incompletely understood. Many BH3 peptide ligands bind indiscriminately to both of these proteins, although efforts to develop small-molecule protein-interaction inhibitors have succeeded for Bcl-x_L but not yet for Mcl-1. Our approach generated peptide ligands with the desired interaction specificities, and this method can now be extended to target any pro-survival Bcl-2 protein with counterselection against one or multiple partners. Using a SPOT peptide-binding assay, we also generated a simple and predictive model that describes the Mcl-1 vs. Bcl-x_L binding properties of a large number of Bim-BH3 variants. Below, we discuss aspects of the yeast screening, the SPOT arrays and the model building, and we provide a rationale for how specificity was achieved in the Mcl-1 vs. Bcl-x_L selective sequences.

Screening for specific binding peptides

To identify specific BH3 peptides, we used a two-tiered approach, combining screening for binding to the preferred pro-survival protein with counter-screening against the undesired interaction partner. Schemes where positive and negative screening are carried out simultaneously have been used in earlier studies to confer specificity on enzymatic reactions using ultrahigh-throughput FACS based methods.[33; 34; 35] In this work, we used sequential sorting of binding-positive and binding-negative clones to identify intermediate pools of sequences for analysis. In this way, we observed that screening for affinity alone enriched a pool of Mcl-1 binding peptides that showed significantly reduced binding to Bcl-x_L (Supplemental Figure 3A, B). Counter screening against Bcl-x_L led to isolation of those Mcl-1

specific clones that did not bind to Bcl-x_L at micromolar concentration, and the majority of these also did not bind to other pro-survival proteins, i.e. Bcl-2, Bcl-w or Bfl-1. Bcl-x_L is more closely related to Bcl-w and Bcl-2 than to Mcl-1 (sequence identities of 38.8%, 47% and 16.7% respectively), so counter-screening against Bcl-x_L may serve to confer specificity against Bcl-2 and Bcl-w. In contrast to the results for Mcl-1, screening for peptides that bound Bcl-x_L in preference to Mcl-1 did not confer specificity prior to counter-screening against Mcl-1 (Supplemental Figure 3C, D). Also, most Bcl-x_L specific clones cross-reacted with Bcl-2 and Bcl-w, although they bound these proteins more weakly than they bound to Bcl-x_L (Figure 3C).

To our knowledge, this is the first screen involving BH3 peptides that introduces specificity as a major criterion. A recent affinity based phage display screen provided a peptide that bound human Mcl-1 with a K_d of ~69 nM and was selective for binding to human and mouse Mcl-1 over Bcl-x_L, Bcl-2 and Bcl-w.[36] Further optimization of this sequence led to a peptide that bound with higher affinity to human Mcl-1 (~ 23 nM) but also bound to Bcl-w (~43 nM). By incorporating specificity criteria directly in our screens, we generated peptides that bound Mcl-1 with low nanomolar affinity and were selective over the other four pro-survival proteins, including Bfl-1, which was not tested with sequences identified by phage display. The phage display screen was done using a randomized 16-mer peptide library. Interestingly, the sequences of the high affinity peptides shared a strong signature that is characteristic of native BH3 motifs, even though such sequences were rare in the library. This suggests that a library that diversifies a known BH3 scaffold, as we have used here, may access more functional diversity.

Comprehensive substitution analysis of Bim-BH3

Mutational studies have been used to probe sequence-structure-function relationships for Bcl-2 family interactions. Published studies have involved alanine and hydrophile scanning of interface positions, and also substitution of 18 amino acids at two hydrophobic sites (3a and 4a) in Bim-BH3.[16; 18; 19; 20; 21] These studies have provided important insights into binding and specificity determinants. Here, we used SPOT arrays to explore BH3 peptide binding even more comprehensively, probing the influence of 170 point mutations in the context of Bim-BH3. Our SPOT array results for Mcl-1 and Bcl-x_L are consistent with previously reported mutagenesis studies and therefore can be used to address the effects of a more comprehensive set of substitutions.[16; 18; 19] Summarizing the trends in Figure 5, we found three positions where substitutions were better tolerated for Mcl-1 binding (2e, 3b and 4a) and three where substitutions were better tolerated for Bcl-x_L binding (2d, 3d and 3e). Certain mutations at position 3a also gave differential effects on Mcl-1 vs. Bcl-x_L binding. In addition to providing a more complete classification of how mutations in Bim-BH3 affect Mcl-1 and Bcl-x_L binding, our comprehensive data set makes it possible to develop a scoring scheme for Bim-like BH3 peptide binding and interaction specificity.

A simple PSSM model

We used the substitution arrays to construct a PSSM and showed that this model can separate Mcl-1 specific sequences from Bcl-x_L specific sequences and from sequences of peptides that bind with high affinity to both receptors (Figure 6E). Thus, although we cannot rule out synergistic effects between positions in Bim-BH3 that may influence binding, much of the specificity observed in the sequences from yeast-display screening can be explained by a simple, linear and additive model. Importantly, this model was derived independent of knowledge of these sequences.

To see if the Bim-BH3-based PSSM could be improved, and to explore the effects of point mutations in the context of sequences selected from the yeast-display library rather than Bim-

BH3, we used the library arrays (Figure 6A, B; Supplemental Figure 7). The PSSM model built using data from the library arrays was similar to that based on the Bim-BH3 substitution analysis, but it did a better job of discriminating high vs. low affinity binding to Mcl-1. We traced this effect largely to the role of stabilizing mutations at position 4a, and confirmed using solution binding studies that Val at this site is stabilizing relative to wild-type Phe for Mcl-1 binding (Figure 6C, D).

The two PSSM models differed in two ways. First, the library arrays allowed us to evaluate the effects of key point substitutions using average values collected over many Bim-like sequences. These averages may provide better estimates of the influence of mutations in the engineered peptides, and the larger numbers of measurements also make them less sensitive to noise. Second, the high affinity of native Bim-BH3 for Mcl-1 and Bcl-x_L saturates the signal in the SPOT arrays for many sequences and thus masks the effects of stabilizing mutations. Because of this, the Bim-BH3 substitution array matrix incorrectly assigned similar weights to Val and Phe at position 4a for Mcl-1 binding. Our work indicates that both the concentration used for the SPOT experiments (compare Figure 5A, B with C, D) and the sequence context in which mutations are made (Figure 6A, B) can be important for providing appropriate mutational data to parameterize a predictive model.

Understanding Mcl-1 vs. Bcl-x_L specificity

Using the SPOT data as a guide, we investigated the mechanisms used to establish interaction specificity in the peptides identified by yeast display. We defined three classes of substitutions according to interaction weights from the arrays (Table 1). Class 1 and 2 substitutions were specific for one pro-survival protein over another. The difference between these two classes is that class 1 substitutions retained strong binding to the desired target on the arrays, whereas class 2 substitutions achieved specificity at the expense of some stability. Class 3 substitutions were highly destabilizing for binding to both pro-survival proteins, without any discernable preference.

Interestingly, most of the substitutions identified as class 1 based on the arrays were highly represented in the specific sequences identified by yeast-display screening, as reflected in the sequence logos in Figure 2. Many class 1 substitutions occurred in positions 3d or 4a (compare Table 1 and Figure 2). At position 3d, both Mcl-1-specific sequences and sequences of peptides that bound both receptors were largely constrained to the wild-type Bim residue Ile. In contrast, sequences specific for Bcl-x_L spanned a range of residues, including polar residues, but never Ile. In co-crystal structures of Bim in complex with Bcl-x_L vs. Mcl-1, the 3d site is less tightly packed in Bcl-x_L, where it is located next to a less helical α2/α3 region of the receptor; this may explain the observed permissiveness.[7] Thus, the class 1 mutations favoring Bcl-x_L at 3d (Ala, Asp, Asn, Phe, Tyr, Thr) appear to be key specificity determining factors disfavoring Mcl-1 binding. At position 4a, the sequence logos in Figure 2E emphasize that Bcl-x_L is selective for large aromatics while Mcl-1 can accommodate multiple substitutions (Figure 2D), with Asn, Ser, Val, Thr and Ile assigned as class 1 mutations favoring Mcl-1 binding. The co-crystal structure of Mcl-1 with the specific peptide MB7 shows that Asn can be easily accommodated at position 4a, without any significant local perturbation, in agreement with previous observations that this site is more open and solvent-exposed in Mcl-1 compared to Bcl-x_L (Figure 4B).[16; 18; 19 31] At position 2d, two class 1 mutations favoring Bcl-x_L (Phe and Tyr) were very common in Bcl-x_L specific sequences (Figure 2E). It is interesting that the BH3 region of Bad, which is highly specific for Bcl-x_L over Mcl-1, also has a Tyr at the same position. Mutational studies in Bad confirm that this residue influences binding specificity.[26] Ile at 3a is a class 1 substitution for Mcl-1, and this is prominent in the Mcl-1-specific sequence logo. The structure in Figure 4a shows how this β-branched residue, universally conserved as Leu in native BH3 sequences, is accommodated in Mcl-1. For position 3b, the sequence logo

reveals relatively low information (Figure 2D, E). However, the substitutions Asn (class 1 for Mcl-1) and Glu or Asp (class 2 for Mcl-1) are present in the Mcl-1 specific sequences and completely absent from the Bcl-x_L specific sequences (Supplemental Tables 3 and 4).

An examination of individual sequences identified in the yeast screen shows that all contain more than one substitution from wild-type Bim-BH3; single mutants did not survive our criteria (binding to the desired receptor at 10 nM and negligible binding to the undesired receptor at 1 μM). This agrees with the observation that most single class 1 substitutions bound the undesired receptor at 1 μM concentration on SPOT membranes. Most Bcl-x_L and some Mcl-1 specific peptides combined multiple class 1 mutations, including Bcl-x_L specific peptide XD5 (two class 1 substitutions: Tyr at position 2d and Asn at position 3d) and Mcl-1 specific MB9 (two class 1 substitutions: Ile at position 3a and Thr at position 4a) (Supplemental Tables 3 and 4). Interestingly, many Mcl-1 specific sequences combined class 1 with class 2/3 substitutions (such as Asp/Glu at position 3b or Asn/Glu at position 3f), thereby achieving specificity but sacrificing stability (Supplemental Table 3). Many of these sequences also included Val/Ile at position 4a as the class 1 mutation. Therefore, we speculated that Val/Ile, in addition to providing specificity as class 1 substitutions, might provide stability to compensate for destabilizing mutations. Interestingly, as shown in Figure 6, the point mutation Phe4aVal in Bim-BH3 increased Mcl-1 binding affinity and conferred a significant preference for binding Mcl-1 over Bcl-x_L. This type of single amino-acid substitution would be missed in our screen, which eliminated all clones that bound Bcl-x_L at 1 μM concentration. These observations point to an interesting strategy to satisfy the requirements of the screen, i.e. combining substitutions that destabilize binding for both receptors (to meet the specificity constraint) with ones that selectively enhance binding for the receptor of interest (to meet the stability constraint). Using the above analysis, we could rationalize the sequence patterns for most of the specific sequences.

We would like to emphasize that the classifications and interpretations presented above are based largely on SPOT experiments but not more rigorous quantitative measurements of binding affinity. Therefore, we avoid some of the more subtle issues, such as the role of substitutions that are not clear-cut in our classification scheme, and questions about whether multiple specificity determinants are synergistic or simply additive. Despite these simplifications, we show that a framework based on a simple SPOT/PSSM analysis can logically explain many sequence-function relationships that underlie the observed behavior of the specific peptides. Whereas our model is imperfect and leaves the detailed behavior of various examples unexplained, the power of experimental screening has nevertheless provided sequences that combine different substitutions to achieve multiple objectives, whether these combinations follow our intuition or have more subtle effects.

Conclusions

In this work, SPOT peptide arrays and yeast-display screening were combined to give a broad overview of specificity determinants in Bim-BH3-based peptides. These two techniques share the advantage that large numbers of interactions can be characterized without laborious synthesis or purification of individual peptides. The approaches are complementary, in that screening of libraries displayed on yeast can identify peptides meeting certain requirements, while SPOT arrays provide a means of systematically perturbing local sequence and testing hypotheses. Here, the combination provided many specific Mcl-1 vs. Bcl-x_L binding peptides (and vice versa), as well as a model for the origins of the binding specificity. Our approach is very general, and can be applied in the future to identify further BH3-like peptides with diverse characteristics. Through these means, a comprehensive understanding of BH3-peptide binding to Bcl-2 family receptors appears within reach.

We are optimistic that these or other peptides engineered for binding specificity may prove useful as reagents. For example, engineered BH3 peptides with selective binding profiles can be used as tools to dissect apoptotic pathways inside cells, where the mechanisms of apoptotic regulation by the Bcl-2 family remain controversial. Selective BH3 peptides can also be used for BH3 profiling, a technique in which treatment with a panel of specific peptides can provide information about the dependency of primary cancer cells on specific Bcl-2 proteins for survival.[14; 37] Selective BH3 peptides may be also modified using "hydrocarbon stapling" for improved pharmacologic properties such as protease resistance and cell permeability.[38] Open questions about whether specific or broad-spectrum Bcl-2 inhibitors have greater value for therapy will not be fully answered until molecules of both types are available. It is our expectation that a better understanding of Bcl-2 family molecular recognition will accelerate the development of such reagents.

Materials and Methods

Yeast strains, media and chemical reagents

Yeast strain EBY100 and the plasmid for yeast surface display (pCTCON2) were a generous gift from Dr. K. D. Wittrup (M.I.T.). Yeast cells were grown in selection media containing glucose (SD-CAA) or galactose (SG-CAA) following published protocols.[39] Antibodies for labeling were purchased from Sigma.

Expression of recombinant pro-survival Bcl-2 proteins

Pro-survival Bcl-2 proteins with a c-myc tag at the amino terminus were used for all studies, with the exception of yeast-display screening experiments involving Bcl-x_L, where an amino terminal His-tagged protein was used. Hexa-His-tagged human Bcl-x_L (residues 1-209) was expressed in Escherichia coli BL21(DE3) and purified as described previously for murine Bcl-x_L.27 All c-myc tagged Bcl-2 proteins were expressed in E. coli BL21(DE3) strains using a modified pSV282 vector (pSVM).[27] This vector was generated to express the Bcl-2 proteins as maltose binding protein (MBP) fusions, which upon tobacco etch virus (TEV) protease cleavage yield an N-terminally c-myc-tagged protein no longer fused to MBP. Human Mcl-1 (residues 172-327), Bcl-x_L (residues 1-209), Bcl-2 (residues 1-217), Bcl-w (residues 1-164) and Bfl-1 (residues 1-151) were purified as follows: Cells were suspended in lysis buffer (20 mM Tris, 100 mM NaCl, pH 8.0). Hen egg lysozyme was added to the suspension to a final concentration of 1 mg/ml and incubated at 37 °C for 20-30 minutes, following which the solution was sonicated ten times for 30 seconds each. Cell debris was removed by centrifugation and sodium chloride was added to the supernatant to a final concentration of 0.5 M. The supernatant was applied to a Ni-NTA agarose (Qiagen) column, equilibrated in Tris buffer (20 mM Tris, 500 mM NaCl, pH 8.0). After washing the column, the His-tagged MBP fusion protein was eluted with buffer containing 500 mM imidazole. Eluted fractions were pooled and dialyzed against TEV cleavage buffer (50 mM Tris, 50 mM NaCl, 0.5 mM EDTA, 1 mM DTT, pH 8.0) overnight at 4 °C. The dialyzed MBP fusions at 1mg/ml were mixed with TEV protease at a ratio of 50:1 (w/w) and incubated overnight at room temperature. The TEV-cleaved reaction mix was centrifuged to remove any insoluble precipitate and purified using a second Ni-NTA column to separate the c-myc tagged Bcl-2 protein from His-tagged MBP and His-tagged TEV protease. Bcl-x_L and Mcl-1 were >95% pure by Coomassie-stained SDS-PAGE after this step. Bcl-2 and Bcl-w were further purified using gel-filtration chromatography with a Sephacryl S-200 column (GE Healthcare) and Bfl-1 was purified over cation exchange resin (Q sepharose Fast Flow, Sigma-Aldrich) by eluting in 50 mM Tris buffer (pH 7.5, 400 mM NaCl). The oligomerization state of each protein after purification was analyzed using a Superdex S75 column (GE Healthcare) in 20 mM Tris, 300 mM NaCl, 10% glycerol, pH 8. With the exception of Bcl-w, all proteins were predominantly monomeric, the monomeric fraction ranging from ~85-100%. Purified Bcl-w consisted of both monomeric

(~42%) and oligomeric fractions (~58%). Untagged human Mcl-1 used for crystallography was purified as described previously and concentrated to ~10 mg/ml using an Amicon concentrator (Millipore, 10 kDa cutoff).[27]

Construction of the yeast-display vector and the combinatorial library

DNA encoding Bim-BH3 (residues 83-113 from human Bim_L) with a carboxy-terminal FLAG tag with flanking BamH1 and Xho1 sites was subcloned into the plasmid pCTCON2,[39] such that Bim-BH3 was fused in-frame to the C terminus of Aga2p with a $(Gly_4\text{-}Ser)_3$ linker. The BH3 peptide library was constructed using homologous recombination in yeast. Wild-type Bim-BH3 was used as a template. The gene was randomized using PCR with mutagenic primers; library positions were randomized using a mutagenic forward primer (5′ GGCCGTCCGGAAATTTGG DHT GCGCAGGAA NYT VRK CGT DHT GGC VRK GAA DHT AATGCGTATTATGCGCGTCGC 3′, where N represents a mixture of A, T, G and C; Y a mixture of C and T; V a mixture of A, C and G; D a mixture of A, G and T; H represents a mixture of A, C and T; R a mixture of A and G; K a mixture of G and T) and a reverse primer (5′ CTAAAAGTACAGTGGGAACAAAGTCG 3′). The PCR product was further amplified to extend the overlapping ends by more than 50 base pairs, as this has been reported to yield the highest number of transformants.[40] The acceptor vector was cleaved with Xho1 and Nhe1 and transformed along with the extended PCR product into yeast following the procedure of Gietz et al.41 After transformation, DNA from a mix of pooled library cells was PCR amplified to check for randomization.

Flow cytometric analysis and sorting

Labeled yeast cells were analyzed on a BD FACScan flow cytometer powered by CellQuest software. The yeast cell population was gated by forward light scatter to avoid analysis of clumped cells. Typically, data for 10,000 events were collected for analysis. For sorting, ~2×10^7 cells (~20 times the library size) were divided into 20 tubes each containing 10^6 cells, and incubated with Bcl-x_L or Mcl-1 for ~60 minutes at room temperature in TBS (50 mM Tris, 100 mM NaCl, pH 8.0). The cells were then pooled into two tubes, centrifuged at ~11,000 rpm and washed with cold TBS. The cells in each tube (~10^7 each) were labeled with primary antibodies (anti-FLAG rabbit and anti-His mouse or anti-c-myc mouse, Sigma) at 1:100 dilution in a volume of 200 μl for a period of 45-60 minutes in BSS (50mM Tris, 100mM NaCl, pH 8, 1mg/ml BSA). This was followed by another round of washing with cold BSS and further labeling of the cells using fluorescein-conjugated (FITC) goat anti-rabbit antibody and R-Phycoerythrein (PE)-conjugated goat anti-mouse IgG (Sigma) secondary antibodies at 1:100 dilution for a period of 45-60 minutes. Following this second round of labeling, cells were again washed with BSS and finally suspended in 500 μl of BSS at a concentration of ~4×10^7 cells/ml for sorting. The sorted cells were collected in selective media containing glucose (SD+CAA) and grown to an O.D. of 6-10 for ~48 hours in the presence of streptomycin/penicillin to prevent bacterial growth. Quantitative equilibrium binding experiments for yeast displayed BH3 peptides with Bcl-x_L or Mcl-1 were performed as described.[23]

Fluorescence polarization binding assays

All unlabelled peptides were synthesized by the M.I.T. Biopolymers facility of the Koch Institute of Integrative Cancer Research. FITC labeled Bim-BH3 was purchased from CHI Scientific. All peptides with sequences given in Figure 3C, except Bcl-x_L specific peptides XG10 and XD5, were synthesized with N-acetylated and C-amidated ends. XG10 and XD5 had free amino and carboxyl termini (for enhanced solubility). Peptides were either purchased > 95% pure or purified by reverse phase HPLC using a C18 column and a linear water/acetonitrile gradient. All fluorescence polarization experiments were done at 25 °C with a FITC labeled 23 residue Bim-BH3 peptide (residues 83-105) in assay buffer (20 mM $NaPO_4$, 50 mM

NaCl, 1 mM EDTA, 0.001% triton X (v/v), 5% DMSO (v/v), pH 7.8). In all binding assays the concentration of FITC-Bim-BH3 measured by amino-acid analysis of a parent stock was 10 nM and the concentration of the pro-survival proteins for the competition binding assays was 50 nM. In each assay, the signal from free labeled peptide (i.e. FITC-Bim-BH3) and bound labeled peptide (i.e. FITC Bim-BH3 with pro-survival protein only) were measured to determine the expected baseline signals. For competition binding assays with Bcl-x_L, peptides were diluted serially in 96 well plates. FITC-Bim-BH3 and Bcl-x_L were premixed and added to each well to a total volume of 120 μL. The plates were covered with aluminum foil and mixed by shaking at 25 °C for 3 hours before the final measurement. A similar procedure was followed for Bcl-2, Bcl-w and Bfl-1. However, premixing FITC-Bim-BH3 with Mcl-1 led to very slow equilibration. Therefore we first premixed the peptides with Mcl-1 in the 96-well plate and then added FITC-Bim-BH3 followed by overnight mixing at 37 °C. The plates were then brought back to room temperature before the final measurement. All anisotropy measurements were performed using a Spectramax M5 (Molecular Devices) plate-reader. For all solution binding experiments, time-dependent measurements over 24-48 hours showed no significant changes in anisotropy values.

The K_i values reported were calculated by fitting competition binding curves using a complete competitive binding model that considered depletion of both the labeled and unlabeled ligand[30]. Due to the limited solubility of some of the unlabeled BH3 peptides, a lower baseline could not be obtained at high concentration. For soluble peptides, the lower baseline was equal to that of the free peptide control in the absence of receptor. Thus, the average values of the free peptide controls were used as the lower baseline for peptides with limited solubility. Five parameters were fit: the lower and upper baselines, the inhibition constant (K_i), and the concentrations of fluorescent Bim and the relevant pro-survival protein (because the activities of these species were difficult to determine precisely). The dissociation constant for binding of Bim-BH3 to any pro-survival protein was fixed at a K_d value of 1 nM, because tighter binding could not be accurately determined using direct binding measurements. Each fit was evaluated to make sure that the concentrations of the species were within a physically realistic range. Curve fitting was done using the program Igor Pro 6.02 (Wavemetrics).

SPOT arrays

Peptide array membranes were synthesized at the M.I.T. Biopolymers facility using an Intavis AutoSpot robot (Intavis AG). Peptides were synthesized by Fmoc-protection chemistry following manufacturer instructions, with cycles 1-7 being double coupled and protected, cycles 8-20 being triple coupled and protected, and cycles 21 and higher being quadruple coupled and triple protected. The 26-mer peptides had PEG3 (three ethylene glycol units) at the peptide C-terminus as a linker to the cellulose membrane. For each membrane, a few spots were synthesized using a rink linker to allow for removal of the peptide from the cellulose for verification by mass spectrometry; analysis always validated the presence of the full-length peptide. Procedures for blocking and probing SPOT membranes were modified from Cold Spring Harbor Protocols.[42] Sub-arrays were cut from the intact membrane, hydrated in 100% ethanol, then transferred to TBS (137 mM NaCl, 2.7 mM KCl, 50 mM Tris, pH 7) and incubated at room temperature for 5 minutes. Membranes were then transferred into re-sealable plastic bags with MBS (TBS with 0.2% Tween 20 and 2% dry milk) and incubated at room temperature for 16-18 hours. Following incubation, arrays were rinsed with T-TBS (TBS with 0.05% Tween-20) and then incubated with Bcl-2 probe protein in MBS for 3 hours at room temperature. Membranes were rinsed twice with T-TBS and then incubated with anti-c-myc-Cy3 antibody (Sigma Aldrich C6594) diluted 100-fold in MBS, for one hour at room temperature. Membranes were rinsed with T-TBS and scanned on a Typhoon 9400 (GE Healthcare). Images were analyzed with ImageQuant (GE Healthcare). Intensity was averaged over a circular area that was equal in size for all spots for a given membrane. No background

correction was performed. For quantification, the intensity of a particular spot was normalized to the signal from wild-type Bim-BH3 by dividing the intensity by the average over all wild-type Bim-BH3 intensities on that membrane (e.g. 20 spots for the substitution arrays).

PSSM model

The first PSSM model was constructed using SPOT intensities from the substitution analysis of Bim-BH3. We defined the score for amino acid i at position j binding to a specific pro-survival protein R, $SR_{i,j}$, by taking the logarithm of the ratio of the fluorescence intensity for the corresponding Bim-BH3 point mutant to the intensity of wild-type Bim-BH3 (averaged over all wild-type spots) on the membrane. Sequences from yeast-display screening were then evaluated by summing the scores for individual residues. To construct the second PSSM, spots from the library array that had raw signal > $10^{6.5}$ were used. To score the contribution of residue i at position j, we computed the log of the ratio of the average signal for peptides with residue i at position j to the average signal for peptides with the native Bim-BH3 residue at position j. For residues not included in the library arrays, the substitution array data were used. However, scores for residues that had normalized intensities greater than 1 in the substitution arrays were reduced to 1. In addition, the score for Ile at 4a was assigned the same value as Val at 4a, because Ile was not included in the library SPOTS and Val and Ile had similar scores from the substitution arrays.

Crystallography

Crystals of the Mcl-1—MB7 peptide complex were grown in hanging drops over a reservoir containing 1 M zinc sulfate, 0.1 M imidazole pH 6.8 at room temperature. The protein was concentrated to 5 mg/ml in 20 mM Tris, 100 mM NaCl, 1 mM DTT, pH 8.0 and mixed with peptide at a 1:1 molar ratio. The hanging drops contained 1 μl of complex mixed with 1 μl of reservoir solution. Crystals were cryo-protected by transferring into 25% glycerol in reservoir solution prior to flash freezing. Diffraction data at 2.35 Å were collected at the Advanced Photon Source at the Argonne National Laboratory, NE-CAT beamline 24ID-C (Supplemental Table 6). The data were integrated and scaled using HKL2000[43] and phased by molecular replacement using PHASER[44] with chain A of structure 2PQK as the search model. Iterative rounds of refinement and model building were performed using PHENIX[45] and COOT[46]. The final structure has two complexes in the asymmetric unit with an R_{work} of 22.2% and R_{free} of 27%.

Accession numbers

Coordinates and structure factors for the Mcl-1—MB7 complex have been deposited in the Protein Data Bank with accession number 3KZ0.

Supplementary Material

Refer to Web version on PubMed Central for supplementary material.

Acknowledgments

This work was funded by the National Institute of General Medical Sciences through awards GM084181 and P50-GM68762 and used automated crystallization equipment purchased with National Institutes of Health Shared Instrumentation Grant No. S10RR024526. Structure determination is based upon research conducted at the Advanced Photon Source on the Northeastern Collaborative Access Team beamlines, which are supported by award RR-15301 from the National Center for Research Resources, National Institutes of Health. Use of the Advanced Photon Source is supported by the US Department of Energy, Office of Basic Energy Sciences, under Contract No. DE-AC02-06CH11357. We thank E. Genillo, J. A. Tan, W. Garcia-Beltran, and the staff at the MIT Flow Cytometry Facility for assistance and R. Cook and the MIT Biopolymers Facility for peptide and SPOT array synthesis. We thank members of the Keating laboratory for providing helpful discussions and the Baker and the Bell laboratories for allowing use of equipment. We also thank R. T. Sauer for help with structure refinement.

References

1. Adams JM, Cory S. The Bcl-2 protein family: arbiters of cell survival. Science 1998;281:1322–6. [PubMed: 9735050]
2. Huang DC, Strasser A. BH3-Only proteins-essential initiators of apoptotic cell death. Cell 2000;103:839–42. [PubMed: 11136969]
3. Letai A, Bassik MC, Walensky LD, Sorcinelli MD, Weiler S, Korsmeyer SJ. Distinct BH3 domains either sensitize or activate mitochondrial apoptosis, serving as prototype cancer therapeutics. Cancer Cell 2002;2:183–92. [PubMed: 12242151]
4. Oltersdorf T, Elmore SW, Shoemaker AR, Armstrong RC, Augeri DJ, Belli BA, Bruncko M, Deckwerth TL, Dinges J, Hajduk PJ, Joseph MK, Kitada S, Korsmeyer SJ, Kunzer AR, Letai A, Li C, Mitten MJ, Nettesheim DG, Ng S, Nimmer PM, O'Connor JM, Oleksijew A, Petros AM, Reed JC, Shen W, Tahir SK, Thompson CB, Tomaselli KJ, Wang B, Wendt MD, Zhang H, Fesik SW, Rosenberg SH. An inhibitor of Bcl-2 family proteins induces regression of solid tumours. Nature 2005;435:677–81. [PubMed: 15902208]
5. Tse C, Shoemaker AR, Adickes J, Anderson MG, Chen J, Jin S, Johnson EF, Marsh KC, Mitten MJ, Nimmer P, Roberts L, Tahir SK, Xiao Y, Yang X, Zhang H, Fesik S, Rosenberg SH, Elmore SW. ABT-263: a potent and orally bioavailable Bcl-2 family inhibitor. Cancer Res 2008;68:3421–8. [PubMed: 18451170]
6. Czabotar PE, Lee EF, van Delft MF, Day CL, Smith BJ, Huang DC, Fairlie WD, Hinds MG, Colman PM. Structural insights into the degradation of Mcl-1 induced by BH3 domains. Proc Natl Acad Sci U S A 2007;104:6217–22. [PubMed: 17389404]
7. Liu X, Dai S, Zhu Y, Marrack P, Kappler JW. The structure of a Bcl-xL/Bim fragment complex: implications for Bim function. Immunity 2003;19:341–52. [PubMed: 14499110]
8. Petros AM, Nettesheim DG, Wang Y, Olejniczak ET, Meadows RP, Mack J, Swift K, Matayoshi ED, Zhang H, Thompson CB, Fesik SW. Rationale for Bcl-xL/Bad peptide complex formation from structure, mutagenesis, and biophysical studies. Protein Sci 2000;9:2528–34. [PubMed: 11206074]
9. Willis SN, Adams JM. Life in the balance: how BH3-only proteins induce apoptosis. Curr Opin Cell Biol 2005;17:617–25. [PubMed: 16243507]
10. Willis SN, Chen L, Dewson G, Wei A, Naik E, Fletcher JI, Adams JM, Huang DC. Proapoptotic Bak is sequestered by Mcl-1 and Bcl-xL, but not Bcl-2, until displaced by BH3-only proteins. Genes Dev 2005;19:1294–305. [PubMed: 15901672]
11. Willis SN, Fletcher JI, Kaufmann T, van Delft MF, Chen L, Czabotar PE, Ierino H, Lee EF, Fairlie WD, Bouillet P, Strasser A, Kluck RM, Adams JM, Huang DC. Apoptosis initiated when BH3 ligands engage multiple Bcl-2 homologs, not Bax or Bak. Science 2007;315:856–9. [PubMed: 17289999]
12. Letai AG. Diagnosing and exploiting cancer's addiction to blocks in apoptosis. Nat Rev Cancer 2008;8:121–32. [PubMed: 18202696]
13. Chen L, Willis SN, Wei A, Smith BJ, Fletcher JI, Hinds MG, Colman PM, Day CL, Adams JM, Huang DC. Differential targeting of prosurvival Bcl-2 proteins by their BH3-only ligands allows complementary apoptotic function. Mol Cell 2005;17:393–403. [PubMed: 15694340]
14. Certo M, Del Gaizo Moore V, Nishino M, Wei G, Korsmeyer S, Armstrong SA, Letai A. Mitochondria primed by death signals determine cellular addiction to antiapoptotic BCL-2 family members. Cancer Cell 2006;9:351–65. [PubMed: 16697956]
15. Kuwana T, Bouchier-Hayes L, Chipuk JE, Bonzon C, Sullivan BA, Green DR, Newmeyer DD. BH3 domains of BH3-only proteins differentially regulate Bax-mediated mitochondrial membrane permeabilization both directly and indirectly. Mol Cell 2005;17:525–35. [PubMed: 15721256]
16. Lee EF, Czabotar PE, Smith BJ, Deshayes K, Zobel K, Colman PM, Fairlie WD. Crystal structure of ABT-737 complexed with Bcl-xL: implications for selectivity of antagonists of the Bcl-2 family. Cell Death Differ 2007;14:1711–3. [PubMed: 17572662]
17. van Delft MF, Wei AH, Mason KD, Vandenberg CJ, Chen L, Czabotar PE, Willis SN, Scott CL, Day CL, Cory S, Adams JM, Roberts AW, Huang DC. The BH3 mimetic ABT-737 targets selective Bcl-2 proteins and efficiently induces apoptosis via Bak/Bax if Mcl-1 is neutralized. Cancer Cell 2006;10:389–99. [PubMed: 17097561]

18. Boersma MD, Sadowsky JD, Tomita YA, Gellman SH. Hydrophile scanning as a complement to alanine scanning for exploring and manipulating protein-protein recognition: application to the Bim BH3 domain. Protein Sci 2008;17:1232–40. [PubMed: 18467496]
19. Lee EF, Czabotar PE, van Delft MF, Michalak EM, Boyle MJ, Willis SN, Puthalakath H, Bouillet P, Colman PM, Huang DC, Fairlie WD. A novel BH3 ligand that selectively targets Mcl-1 reveals that apoptosis can proceed without Mcl-1 degradation. J Cell Biol 2008;180:341–55. [PubMed: 18209102]
20. Day CL, Smits C, Fan FC, Lee EF, Fairlie WD, Hinds MG. Structure of the BH3 domains from the p53-inducible BH3-only proteins Noxa and Puma in complex with Mcl-1. J Mol Biol 2008;380:958–71. [PubMed: 18589438]
21. Sattler M, Liang H, Nettesheim D, Meadows RP, Harlan JE, Eberstadt M, Yoon HS, Shuker SB, Chang BS, Minn AJ, Thompson CB, Fesik SW. Structure of Bcl-xL-Bak peptide complex: recognition between regulators of apoptosis. Science 1997;275:983–6. [PubMed: 9020082]
22. Boder ET, Wittrup KD. Yeast surface display for screening combinatorial polypeptide libraries. Nat Biotechnol 1997;15:553–7. [PubMed: 9181578]
23. Boder ET, Wittrup KD. Yeast surface display for directed evolution of protein expression, affinity, and stability. Methods Enzymol 2000;328:430–44. [PubMed: 11075358]
24. Frank R. Spot-synthesis - an easy technique for the positionally addressable, parallel chemical synthesis on a membrane support. Tetrahedron 1992;48:9217–9232.
25. Herman MD, Nyman T, Welin M, Lehtio L, Flodin S, Tresaugues L, Kotenyova T, Flores A, Nordlund P. Completing the family portrait of the anti-apoptotic Bcl-2 proteins: crystal structure of human Bfl-1 in complex with Bim. FEBS Lett 2008;582:3590–4. [PubMed: 18812174]
26. Day CL, Chen L, Richardson SJ, Harrison PJ, Huang DC, Hinds MG. Solution structure of prosurvival Mcl-1 and characterization of its binding by proapoptotic BH3-only ligands. J Biol Chem 2005;280:4738–44. [PubMed: 15550399]
27. Fu X, Apgar JR, Keating AE. Modeling backbone flexibility to achieve sequence diversity: the design of novel alpha-helical ligands for Bcl-xL. J Mol Biol 2007;371:1099–117. [PubMed: 17597151]
28. Crooks GE, Hon G, Chandonia JM, Brenner SE. WebLogo: a sequence logo generator. Genome Res 2004;14:1188–90. [PubMed: 15173120]
29. Zhang H, Nimmer P, Rosenberg SH, Ng SC, Joseph M. Development of a high-throughput fluorescence polarization assay for Bcl-x(L). Anal Biochem 2002;307:70–5. [PubMed: 12137781]
30. Roehrl MH, Wang JY, Wagner G. A general framework for development and data analysis of competitive high-throughput screens for small-molecule inhibitors of protein-protein interactions by fluorescence polarization. Biochemistry 2004;43:16056–66. [PubMed: 15610000]
31. Fire E, Gullá S, Grant RA, Keating AE. Mcl-1- Bim complexes accommodate surprising point mutations via minor structural changes. Protein Sci 2009;19:507–519. [PubMed: 20066663]
32. Smits C, Czabotar PE, Hinds MG, Day CL. Structural plasticity underpins promiscuous binding of the prosurvival protein A1. Structure 2008;16:818–29. [PubMed: 18462686]
33. Antipov E, Cho AE, Wittrup KD, Klibanov AM. Highly L and D enantioselective variants of horseradish peroxidase discovered by an ultrahigh-throughput selection method. Proc Natl Acad Sci U S A 2008;105:17694–9. [PubMed: 19004779]
34. Varadarajan N, Gam J, Olsen MJ, Georgiou G, Iverson BL. Engineering of protease variants exhibiting high catalytic activity and exquisite substrate selectivity. Proc Natl Acad Sci U S A 2005;102:6855–60. [PubMed: 15867160]
35. Varadarajan N, Pogson M, Georgiou G, Iverson BL. Proteases That Can Distinguish among Different Post-translational Forms of Tyrosine Engineered Using Multicolor Flow Cytometry. J Am Chem Soc 2009;131:18186–18190. [PubMed: 19924991]
36. Lee EF, Fedorova A, Zobel K, Boyle MJ, Yang H, Perugini MA, Colman PM, Huang DC, Deshayes K, Fairlie WD. Novel Bcl-2 homology-3 domain-like sequences identified from screening randomized peptide libraries for inhibitors of the pro-survival Bcl-2 proteins. J Biol Chem 2009;284:31315–26. [PubMed: 19748896]
37. Deng J, Carlson N, Takeyama K, Dal Cin P, Shipp M, Letai A. BH3 profiling identifies three distinct classes of apoptotic blocks to predict response to ABT-737 and conventional chemotherapeutic agents. Cancer Cell 2007;12:171–85. [PubMed: 17692808]

38. Walensky LD, Kung AL, Escher I, Malia TJ, Barbuto S, Wright RD, Wagner G, Verdine GL, Korsmeyer SJ. Activation of apoptosis in vivo by a hydrocarbon-stapled BH3 helix. Science 2004;305:1466–70. [PubMed: 15353804]

39. Chao G, Lau WL, Hackel BJ, Sazinsky SL, Lippow SM, Wittrup KD. Isolating and engineering human antibodies using yeast surface display. Nat Protoc 2006;1:755–68. [PubMed: 17406305]

40. Raymond CK, Pownder TA, Sexson SL. General method for plasmid construction using homologous recombination. Biotechniques 1999;26:134–8. 140–1. [PubMed: 9894602]

41. Gietz RD, Woods RA. Transformation of yeast by lithium acetate/single-stranded carrier DNA/polyethylene glycol method. Methods Enzymol 2002;350:87–96. [PubMed: 12073338]

42. Frank, R.; Dubel, S. Cold Spring Harbor Protocols. Vol. 23. 2006. Analysis of Protein Interactions with Immobilized Peptide Arrays Synthesized on Membrane Supports. pdb.prot4566

43. Otwinowski Z, Minor W. Processing of X-ray diffraction data collected in oscillation mode. Macromolecular Crystallography, Pt A 1997;276:307–326.

44. McCoy AJ, Grosse-Kunstleve RW, Adams PD, Winn MD, Storoni LC, Read RJ. Phaser crystallographic software. J Appl Crystallogr 2007;40:658–674. [PubMed: 19461840]

45. Adams PD, Grosse-Kunstleve RW, Hung LW, Ioerger TR, McCoy AJ, Moriarty NW, Read RJ, Sacchettini JC, Sauter NK, Terwilliger TC. PHENIX: building new software for automated crystallographic structure determination. Acta Crystallogr D Biol Crystallogr 2002;58:1948–54. [PubMed: 12393927]

46. Emsley P, Cowtan K. Coot: model-building tools for molecular graphics. Acta Crystallogr D Biol Crystallogr 2004;60:2126–32. [PubMed: 15572765]

Abbreviations used

FACS	Fluorescence Activated Cell Sorting
BH	Bcl-2 homology
FITC	Fluorescein isothiocyanate
PE	R-Phycoerythrein
PSSM	Position-specific scoring matrix

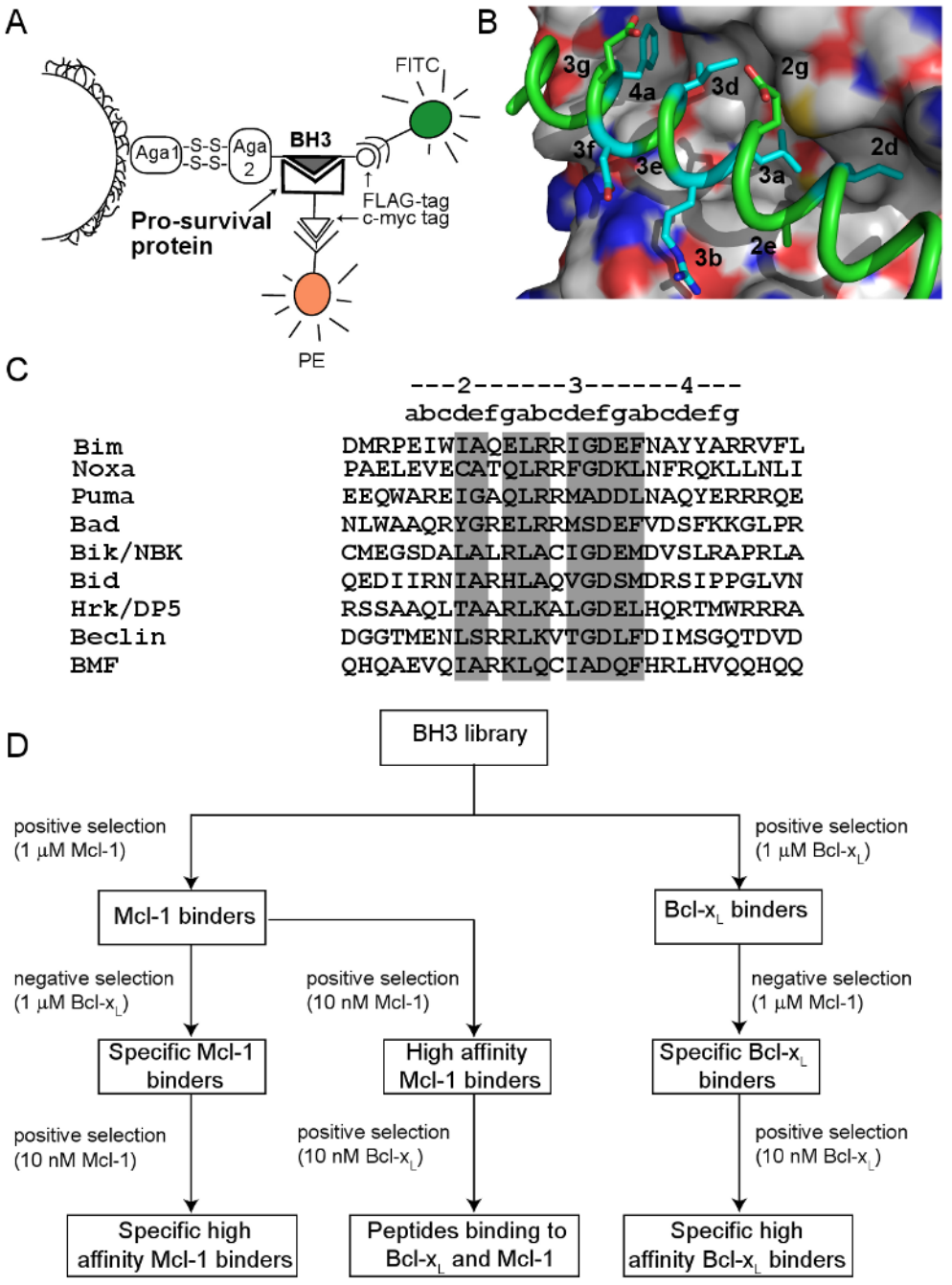

Figure 1.

Screening a combinatorial BH3 peptide library using yeast surface display. (A) Schematic of the yeast-display system used to study interactions of BH3 peptides with pro-survival proteins Bcl-x_L and Mcl-1. Expression of the BH3 peptide as a fusion to the yeast cell surface protein Aga2p was monitored by immunofluorescence detection of a FLAG tag located at the carboxyl terminus of the BH3 peptide (FITC fluorescence); binding of a pro-survival protein (Bcl-x_L or Mcl-1) was monitored by detection of a c-myc tag located at the amino terminus (PE fluorescence). (B) Positions of Bim-BH3 that were varied in the yeast-display or SPOT studies are shown as sticks in a structure of Bim bound to Mcl-1 (PDB code:2PQK). Residues varied in the yeast-display library are in cyan; additional residues substituted in the SPOT arrays are

in green. Mcl-1 is shown using a surface representation. (C) Alignment of representative BH3 sequences from human BH3-only proteins. Residue positions randomized in the yeast-display library or mutated in the SPOT substitution analysis are shaded; numbering using a heptad convention is shown at the top. (D) Schematic of the screening scheme for isolating BH3 peptides with different binding specificities.

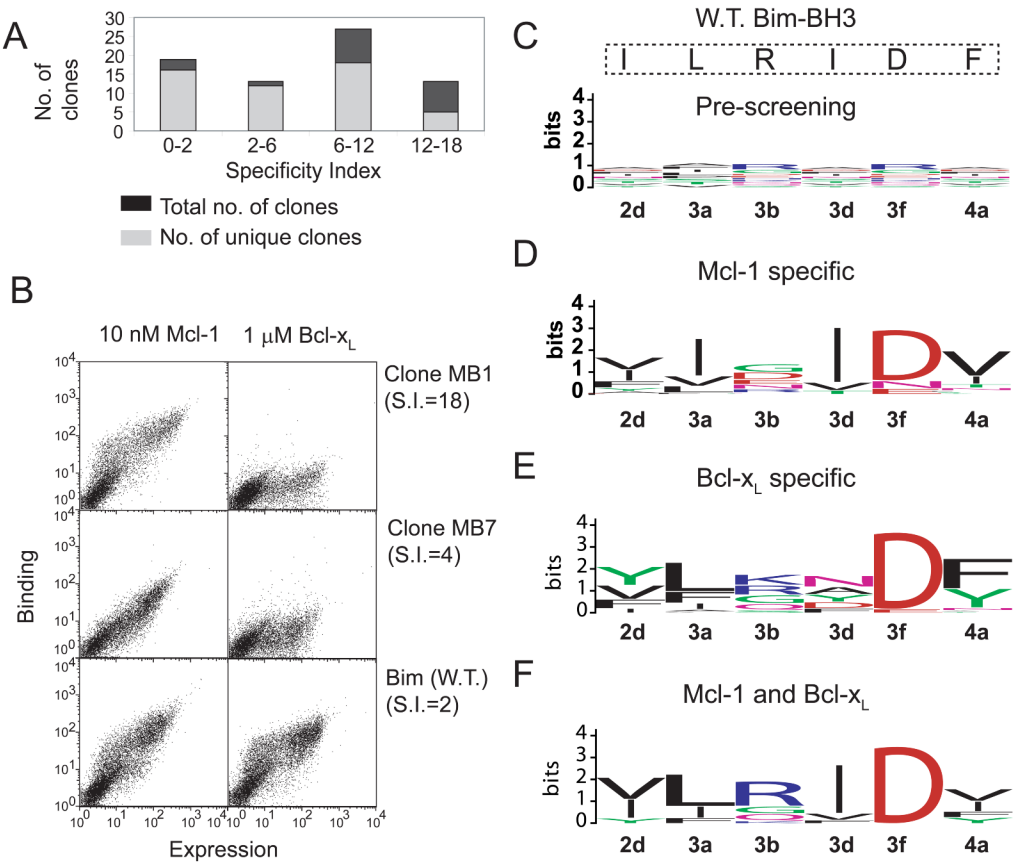

Figure 2.

Characterization of clones from the yeast-display screen. (A) Sequenced Mcl-1 specific peptides are binned according to their specificity indices (S.I.) measured using yeast surface display, where S.I. = (mean fluorescence for binding to 10 nM Mcl-1)/(mean fluorescence for binding to 1 μM Bcl-x_L). (B) Bivariate flow cytometric plots of two Mcl-1 specific clones and wild-type Bim-BH3 are shown with their respective S.I. values. At left, binding in the presence of 10 nM Mcl-1; at right, binding in the presence of 1 μM Bcl-x_L. (C-F) Sequence logos for different populations. In (C), the library prior to sorting with composition weighted by codon degeneracy; wild-type Bim residues are boxed at the top; in (D) Mcl-1 specific peptides; in (E) Bcl-x_L specific peptides; in (F) peptides that bound to both Bcl-x_L and Mcl-1.

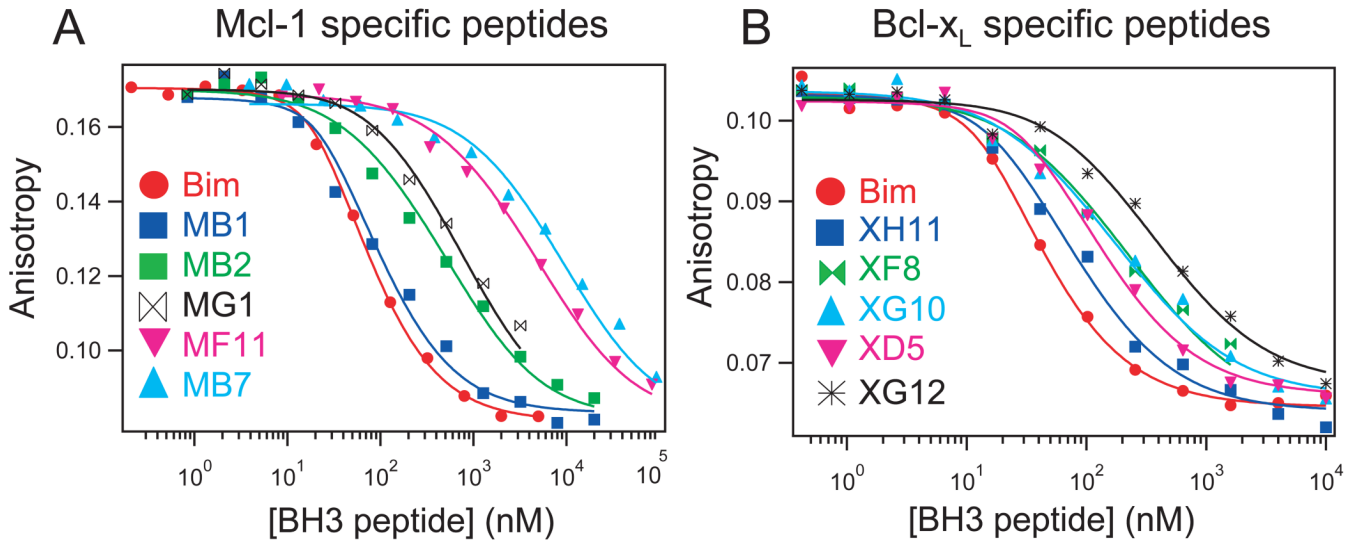

C

Peptide	Sequence	K_i (nM) Bcl-x_L	Bcl-w	Bcl-2	Mcl-1	Bfl-1
Bim	RPEIWIAQELRRIGDEFNAYYAR	1.3 ± 0.4	2.1 ± 0.3	1.4 ± 0.6	1.9 ± 0.3	2 ± 0.1
	Mcl-1 specific peptides					
MB1	RPEIWIAQEIDRIGDEVNAYYAR				4 ± 1.8	
MB2	RPEIWFAQEIDRIGDEVNAYYAR				20 ± 2	
MG1	RPEIWFAQEFSRIGDEVNAYYAR				30 ± 6	
MF11	RPEIWVAQELERIGEEVNAYYAR				192 ± 11	
MB7	RPEIWAAQEIRRIGDENNAYYAR				273 ± 37	
	Bcl-x_L specific peptides					
XH11	RPEIWVAQELKRNGDEFNAYYAR	2.9 ± 0.8	81 ± 11	73 ± 7		
XF8	RPEIWFAQELKRNGDEYNAYYAR	9 ± 2	40 ± 26	132 ± 61		
XG10	RPEIWYAQEIRRFGDEFNAYYAR	13 ± 6	220 ± 44	255 ± 3		
XD5	RPEIWYAQELRRNGDEFNAYYAR	6 ± 1	30 ± 9	137 ± 5		
XG12	RPEIWYAQELGRAGDEFNAYYAR	19 ± 1	109 ± 23	725 ± 249		

K_i < 10 nM 10 nM < K_i < 100 nM 100 nM < K_i < 1000 nM K_i > 1000 nM

Figure 3.

Characterization of specific peptides using an *in vitro* fluorescence polarization assay. Competition of (A) Mcl-1 specific peptides and (B) Bcl-x_L specific peptides with fluorescently labeled Bim-BH3 for binding to Mcl-1 and Bcl-x_L, respectively. Binding curves from representative experiments are shown. The concentration of Bcl-x_L or Mcl-1 was 50 nM. Wild-type Bim-BH3 is shown for comparison. The higher concentration points for Mcl-1 specific peptide MG1 and Bcl-x_L specific peptide XF8 were excluded due to low solubility, which led to light scattering (see materials and methods for additional notes about curve fitting). (C) Inhibition constants for Bim-BH3 and selected Mcl-1 and Bcl-x_L specific peptides measured using the competition binding assay. Average values from a minimum of two experiments are shown with errors as standard deviations over replicates.

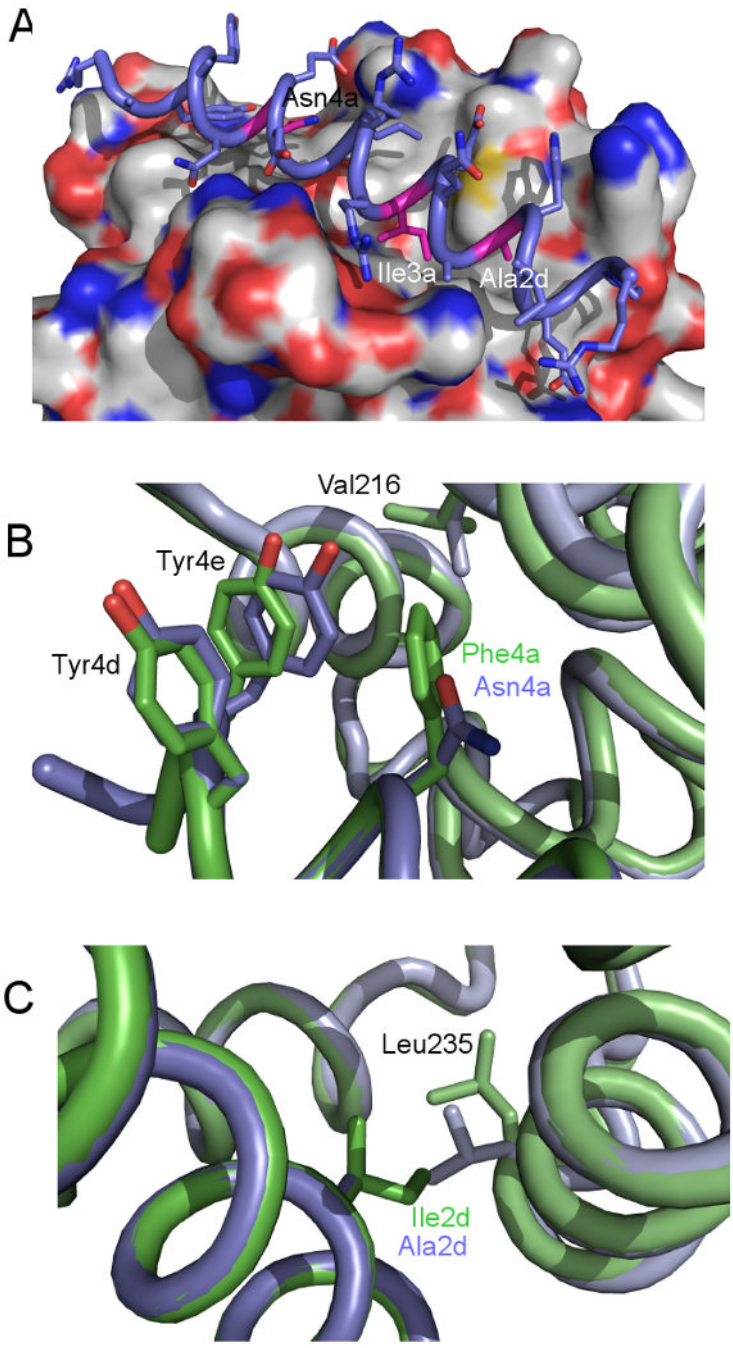

Figure 4.

X-ray structure of Mcl-1 specific peptide MB7 bound to Mcl-1. (A) Close up of the hydrophobic groove of human Mcl-1 (surface), with the MB7 peptide helix in slate blue. Residues that differ from wild-type Bim-BH3 are labeled. Small structural differences with respect to the structure of a wild-type Bim-BH3—Mcl-1 complex are observed in the vicinity of position 4a (B) and 2d (C). The MB7 complex is in blue and the native Bim-BH3 complex is in green (PDB entry: 2PQK).

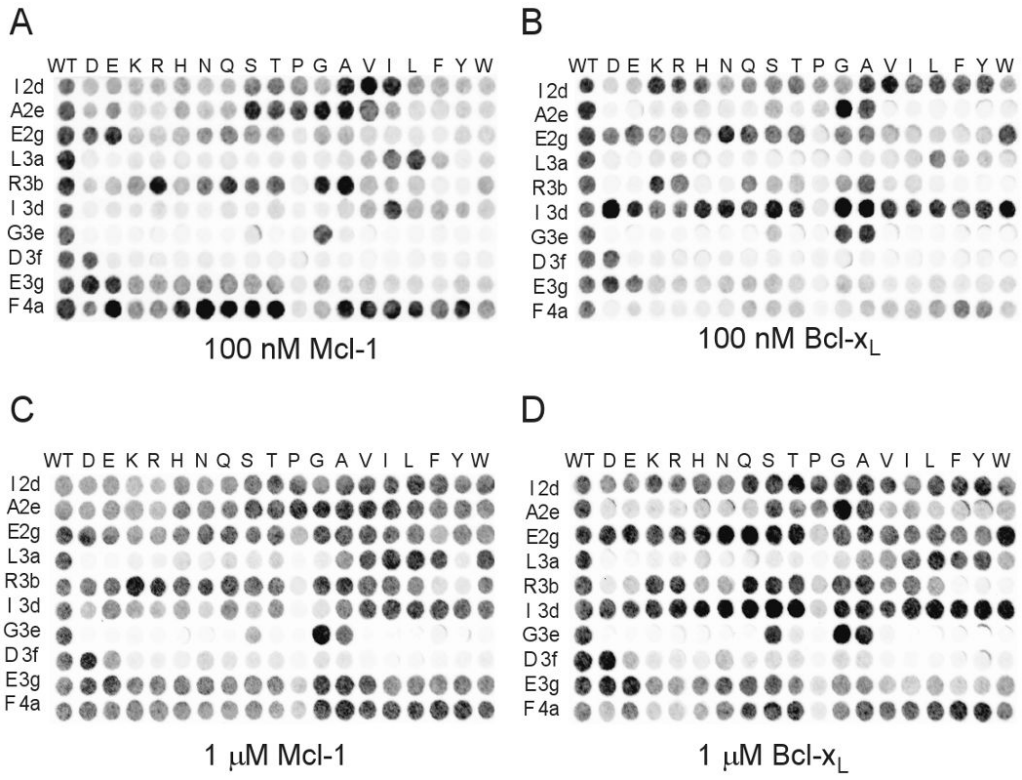

Figure 5.

SPOT array substitution analysis of Bim-BH3 peptides binding to Mcl-1 and Bcl-x_L. Data are for Mcl-1 binding in (A) and (C) and for Bcl-x_L binding in (B) and (D). The top and bottom panels used 100 nM and 1 μM protein, respectively. All spots in the leftmost column of each membrane show binding to the wild-type Bim-BH3 peptide. All other spots are point substitutions or a single repeat of the wild-type sequence in each row, with rows defining residue positions and columns indicating residue identities.

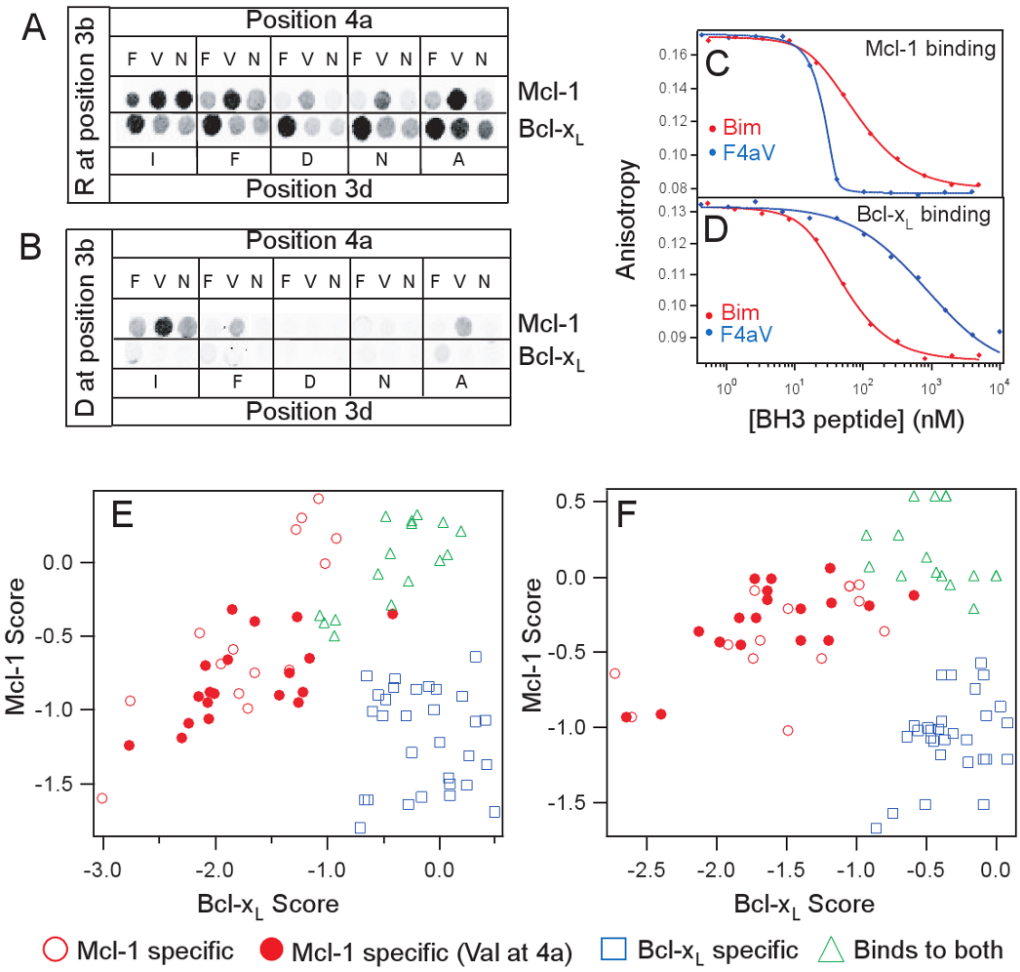

Figure 6.

A model built using the SPOT array data captures the specificities of sequences identified using yeast display. (A and B) A section of the library arrays showing position 4a substitutions. (A) Each boxed set of three spots shows substitution at position 4a with Phe, Val or Asn. Mutations were made with different residues at position 3d, as indicated, with all other residues identical to wild-type Bim-BH3. SPOTS in the top or bottom rows were probed with 100 nM Mcl-1 or 100 nM Bcl-x_L, respectively. (B) Same as (A) but for mutations made in the context of Asp at 3b. (C) Effect of a Phe-to-Val substitution at position 4a in Bim-BH3 on binding to Mcl-1 (C) or Bcl-x_L (D) in fluorescence competition binding assays as described in Figure 3. (E) Engineered BH3 peptide sequences from the yeast screen were scored using a PSSM based on the Bim-BH3 substitution array data. The points plotted correspond to: Mcl-1 specific peptides (red circles), Mcl-1 specific peptides with Val at position 4a (red filled circles); Bcl-x_L specific peptides (blue squares), peptides that bound to both proteins (green triangles). (F) The same plot constructed with a PSSM that included the SPOT library array data; this model gave better separation of Mcl-1 binders vs. non-binders along the Mcl-1 score axis.

Table 1

Classification of representative substitutions observed in selected sequences according to their intensities as measured on the substitution SPOT array.

Position	Substitutions	Class	Specificity
2d	F/Y	1[a]	Bcl-x_L
3a	I	1[a]	Mcl-1
	A	3[c]	-
3b	N	1[a]	Mcl-1
	D, E	2[b]	Mcl-1
3d	A/D/N/F/Y/T/V	1[a]	Bcl-x_L
3f	E/N	3[c]	-
4a	N/S/V/T/I	1[a]	Mcl-1

[a] Normalized signal intensity for binding to one receptor more than 2 fold of that of another. Signal intensity for the preferred receptor (>= 0.7)

[b] Normalized signal intensity for binding to one receptor more than 2 fold of that of another. Signal intensity for the preferred receptor (~0.2-0.3)

[c] Normalized signal intensities for both receptors < 0.2